A study of the tautomers of *N*-salicylidene-*p*-X-aniline compounds in methanol

Victor Vargas and Luis Amigo

Laboratory of Luminescence and Molecular Structure, Department of Chemistry, Faculty of Sciences, University of Chile, Casilla 653, Santiago, Chile. E-mail: victor@uchile.cl

Received (in Cambridge, UK) 30th January 2001, Accepted 11th April 2001
First published as an Advance Article on the web 31st May 2001

We have studied the enol-imine→keto-amine tautomeric equilibrium of *N*-salicylidene-*p*-X-aniline compounds with X = Me, OMe, NMe_2 as electron donor substituents and X = COMe, CN and NO_2 as electron acceptor substituents. The equilibrium constants (K°_{tau}) and standard thermodynamic properties ΔG°_{tau}, ΔH°_{tau} and ΔS°_{tau} were measured and calculated in methanol solution at various temperatures, by means of excitation fluorescence spectroscopy. We have analyzed the *p*-phenylaniline substitution effect on K°_{tau} and the thermodynamic properties through the Hammett parameters σ. We have performed molecular orbital calculations at the semiempirical AM1 and *ab initio* HF/3-21G levels to interpret the experimental results, explicitly including the solute–solvent interaction through the formation of an intermolecular hydrogen bond between the salicylidene and methanol molecules. These computational results show a good correlation with the experimental values. An interpretation of the experimental values of $T\Delta S^{\circ}$, based on changes in the molecular structure produced in the enol-imine→keto-amine tautomeric reaction, is proposed.

Introduction

Intramolecular proton transfer reactions in the ground or excited electronic states have been the subject of several experimental and theoretical studies.[1–6] Schiff bases of *N*-salicylidene-*p*-X-aniline are model systems presenting intramolecular proton transfer between the O and N atoms, leading to an enol-imine⇌keto-amine equilibrium, as shown in Fig. 1. This tautomerism, that induces interesting photo- and thermochromism properties,[7] depends on the electronic structure, temperature and the polar nature of the solvent.

In previous studies carried out on 2-hydroxy-1-naphthaldehyde Schiff bases, the tautomeric equilibrium constants, K°_{tau}, were determined by NMR.[8,9] This technique can be used with precision only for similar relative concentrations of the different species in solution.

This paper presents a study of the enol-imine→keto-amine tautomeric reaction of compounds **1**–**7** in methanol solution (see Fig. 1). The equilibrium tautomeric constants (K°_{tau}), and the thermodynamic standard properties, free energy (ΔG°_{tau}), enthalpy (ΔH°_{tau}) and entropy (ΔS°_{tau}), are determined by means of excitation fluorescence spectroscopy.[10] The aim of this paper is to analyze, from experimental and theoretical points of view, the effect of *para* substitution in the phenylaniline ring of *N*-salicylidene-*p*-X-anilines on K_{tau} constants and the thermodynamic properties.

In order to obtain greater insight into the tautomerisation process, we have performed semiempirical AM1 and *ab initio* molecular orbital calculations for the proton transfer reaction. The specific interaction with the solvent is modeled by means of an intermolecular hydrogen bond, for the enol–methanol and keto–methanol systems. Based on these results, we propose an explanation for the experimental values of $T\Delta S^{\circ}$, observed in the enol-imine→keto-amine tautomeric reaction.

N-salicylidene-*p*-X-aniline

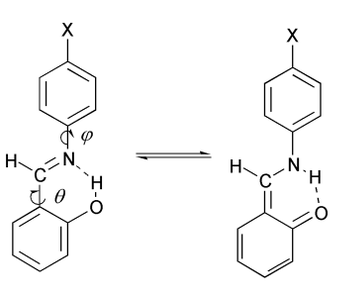

enol-imine

1 X = NO_2
2 X = COMe
3 X = CN

keto-amine

4 X = H
5 X = Me
6 X = OMe
7 X = NMe_2

Fig. 1 The *N*-salicylidene-*p*-X-aniline series studied in this paper.

Experimental and computational methods

Compounds **1**–**7** were synthesized by a condensation procedure, stirring equimolar quantities of salicylaldehyde and the aniline in methanol solution. Double crystallizations were carried out in methanol at low temperature followed by vacuum sublimation. The compounds under study were characterized by IR and ^{1}H-NMR spectroscopy. Solutes and solvents were purchased from Aldrich. Methanol for the emission study was Fischer HPLC grade, with a low fluorescence background.

The absorption spectra were obtained in a Perkin-Elmer Lambda 11 UV-VIS spectrophotometer in a 10 mm quartz cell. Excitation fluorescence spectra, corrected by Rhodamine G, were obtained in the ISS-PC Photon counting spectrofluorometer, coupled to a thermoregulated methanol bath. The total intensity is detected across a 550 nm cut-on filter and the temperature was measured in the cell sample compartment by using an iron-constantan thermocouple.

All the geometric structures for enol- and keto–methanol complexes were optimized by means of the semiempirical molecular orbital AM1 method[11] using the WinMopac package.[12] The enthalpy for the tautomeric reaction (ΔH_{tau}) is directly calculated as the difference of the heat of formation of both tautomers. *Ab initio* calculations were performed with Gaussian 98 software,[13] at the restricted Hartree–Fock level, using the standard 3-21G basis set and fully optimizing the structure of the solute–methanol complex. The frequency option was used for thermodynamic calculations. These

 DOI: 10.1039/b101041g

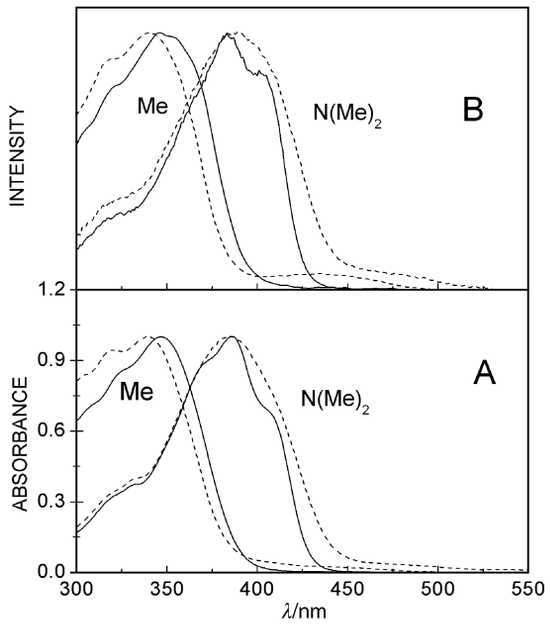

Fig. 2 A. Absorption spectra of compounds **5** (X = Me) and **7** (X = NMe_2), in cyclohexane (——) and methanol (- -) solvent. B. Excitation fluorescence spectra of compound **5** (X = Me) and **7** (X = NMe_2) in cyclohexane (——) and methanol (- -) solvent.

calculations were further improved by extending the basis set to 6-311G* and performing calculations at that level but keeping the optimized 3-21G structures (HF/ 6-311G*// 3-21G).

Results and discussion

a. Spectroscopic results

The absorption spectra of compounds **1**–**7** in solution, in the 300 to 500 nm region, are characterized by a broad and intense band centered at 340 nm. A spectral shift to 380 nm is in agreement with an increasing electron donor strength of the substituents.[14] In Fig. 2-A we compare the absorption spectra of compounds **5** (X = Me) and **7** (X = NMe_2) in methanol and cyclohexane solutions. In methanolic solution, we observe a new weak absorption band in the 450 to 500 nm region, which is absent in cyclohexane solution. The same band was observed by Dudek and Dudek[15] in *N*-salicylidene-*o*-toluidine, when they added small amounts of propionic acid to 3-methylpentane solution. They assign this absorption band to a *cis*-keto-aniline tautomer.

The corrected fluorescence excitation spectra for the same substituted compounds in cyclohexane and methanol solutions are presented in Fig. 2-B. With only slight differences, they recover the absorption spectra presented in Fig. 2-A, *i.e.*, in cyclohexane solutions, we observe only one band with a maximum located within the 340–380 nm region, which can be associated with the enol species. In methanol we observe the enol band plus a low absorption one, in the 450–500 nm region, which is associated with the keto form.

Due to the very high sensitivity of the fluorescence technique, we have used excitation fluorescence spectroscopy to measure with better precision the intensity of the maximum UV and VIS bands. For the low intensity band we have obtained a ratio signal/noise of about 100. Furthermore, since at low optical densities (OD <0.1), the fluorescence intensity is proportional to the sample concentration, we have assumed that for the excitation fluorescence in methanol solution, the maximum intensities of the UV (I_{enol}) and VIS (I_{keto}) bands are proportional to the concentration of the enol and keto species, respectively.

Fig. 3-A presents the excitation fluorescence spectra at different temperatures of compound **5** in methanol solutions.

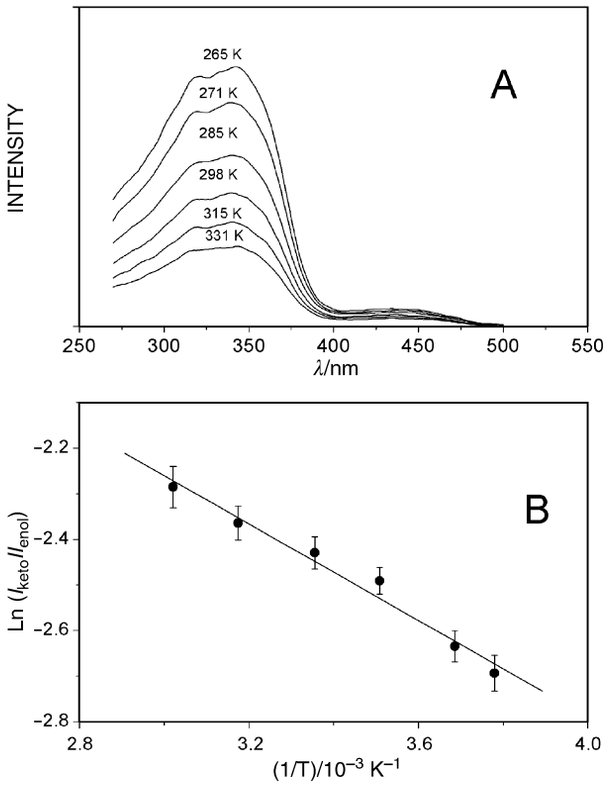

Fig. 3 A. Excitation fluorescence spectra of compound **5** in methanol solution as a function of temperature. B. Logarithmic relationship between I_{keto}/I_{enol} and the reciprocal of the absolute temperature for compound **5** in methanol solution. I_{keto} and I_{enol} were measured from Fig. 3-A spectra at 450 and 345 nm, respectively.

These spectra show decreasing intensity with increasing temperature. This change is more evident in the UV band (330 nm). The other compounds under study present a similar spectral intensity pattern for the UV and VIS bands at different temperatures.

The enol-imine→keto-amine reaction is characterized by the equilibrium tautomeric constants (K°_{tau}) at 298 K. In our experimental scheme, K°_{tau} is calculated from the excitation spectra intensity by eqn. (1), and the free standard energy (ΔG°_{tau}) is calculated by using eqn. (2).

$$K^{\circ}_{tau} = \frac{I_{keto}}{I_{enol}} \quad (1)$$

$$\Delta G^{\circ}_{tau} = -RT \ln K^{\circ}_{tau} \quad (2)$$

The standard enthalpy (ΔH°_{tau}) and standard entropy (ΔS°_{tau}), for the tautomeric reaction are obtained from the linear regression, eqn. (3).

$$\ln\left(\frac{I_{keto}}{I_{enol}}\right) = \frac{-\Delta H^{\circ}_{tau}}{R}\frac{1}{T} + \frac{\Delta S^{\circ}_{tau}}{R} \quad (3)$$

Fig. 3-B shows the plot of $\ln(I_{keto}/I_{enol})$ against the reciprocal of the absolute temperature. For all the compounds in this study, a good linear regression is obtained, which allows the calculation of ΔH°_{tau} and ΔS°_{tau} directly as the slope and the intercept of eqn. (3), respectively.

In Table 1 we display the K°_{tau}, ΔG°_{tau}, ΔH°_{tau} and $-T\Delta S^{\circ}_{tau}$ values obtained with that procedure. We note that these data do not present a large dependence on the variation of the acceptor or donor capacity of the substituents in the phenylaniline group. They do present, however, a clear trend: K°_{tau} decreases and ΔG°_{tau}, ΔH°_{tau} increase when the *para* substituent in the aniline ring goes from the dimethylamine donor group to the nitro acceptor group.

Table 1 Experimental equilibrium tautomeric constants, and standard thermodynamic properties (kJ mol^{-1}) of *N*-salicylidene-*p*-X-aniline in methanol solution

X	σ_p [a]	$10^{-2}\ K^{\circ}_{tau}$	ΔG°_{tau}	ΔH°_{tau}	$-T\Delta S^{\circ}_{tau}$
-NMe_2	−0.63	6.48±1.22	6.78±0.46	3.80±0.21	2.95±0.25
-OMe	−0.28	4.86±0.98	7.49±0.50	5.01±0.17	2.48±0.25
-Me	−0.14	7.23±1.53	6.49±0.52	4.55±0.31	1.94±0.15
-H	−0.00	5.73±1.31	7.08±0.56	5.25±0.30	1.88±0.21
-COMe	0.47	3.00±0.82	8.68±0.67	6.25±0.38	2.43±0.25
-CN	0.70	2.04±0.61	9.64±0.73	7.10±0.57	2.53±0.27
-NO_2	0.81	2.19±0.62	9.46±0.70	6.37±0.44	3.08±0.41

[a] From ref. 17.

In Table 1 we also display the standard entropy values. Note that the enol→keto tautomeric reaction has an important entropy contribution at 298 K (20–40% of the free standard energy). This contribution is higher in more polar substituted compounds (NMe_2 and NO_2) than in less polar compounds. These entropy values will be discussed later along with the results of the computational calculations.

b. Hammett analysis

In order to characterize the substituent effect on K°_{tau} and thermodynamic properties, we used the Hammett analysis, where σ_p, the Hammett parameter, is related to K°_{tau} through eqn. (4).[16]

$$\log K^{\circ}_{tau} = \rho\sigma_p + \log K^{H}_{tau} \qquad (4)$$

In this equation, K^{H}_{tau} is the equilibrium tautomeric constant for *N*-salicylidene-*p*-X-aniline, and ρ, the reaction constant, is the slope appearing in the log K°_{tau} *vs.* σ_p plot. Fig. 4-A shows a good correlation of log K°_{tau} with σ_p[17] ($r = 0.91$). The ρ and log K^{H}_{tau} constants are −0.38±0.08 and −1.34±0.25, respectively; the latter value is in good agreement with that for log K°_{tau} for the unsubstituted system determined from Table 1.

The reaction constants ρ have been interpreted as a measure of the sensitivity of the equilibrium to the electronic substituent effect, which is, by definition, 1.00 for the dissociation of benzoic acid in water at 25 °C.[16] If $\rho > 0$, the electron acceptor substituent favours the right hand of the equilibrium equation. For the salicylidene compounds $\rho < 0$, thereby indicating that an electron acceptor favours the left side of the equilibrium, *i.e.*, the enol species. An electron donating substituent favours the right hand side of the equilibrium reaction, *i.e.*, the keto species. On the other hand, small values of ρ can be interpreted as a low sensitivity of the tautomeric equilibrium to the substituent effects, probably due to lower through-bond interactions with the OH group.

Fig. 4 also includes the correlation of Hammett parameters with the standard free energy (Fig. 4-B) and enthalpy (Fig. 4-C), respectively. We have found the values 2.20±0.47, 7.65±0.23 for the slope and intercept in ΔG°_{tau}, and 2.03±0.30, 5.22±0.15 in ΔH°_{tau}, respectively. These relationships found for ΔG°_{tau} and ΔH°_{tau} with the σ_p parameters suggest that the entropic changes in the tautomeric reaction present a linear dependence with the Hammett parameter of the substituent, ($-T\Delta S^{\circ}_{tau} = 0.2\sigma_p + 2.4$). Due to the small value of the slope (close to zero) the experimental entropic changes in the salicylidene derivatives could not be explained solely on the basis of the electronic nature of the substituent (see Table 1).

c. Molecular orbital calculations

Formation of the hydrogen bonded complex. To interpret the experimental results, we have used the semiempirical AM1 method and the *ab initio* Hartree–Fock method to estimate the thermodynamic standard functions ΔH°, ΔG° and ΔS°. In both calculations we have assumed that the specific solute–solvent interaction can be described by means of an intermolecular hydrogen bond between the solute and a methanol molecule (solute–methanol hydrogen bonded complex). Fig. 5 shows the interaction between the solute molecule, in both tautomeric forms with methanol. Fig. 6 displays the optimized geometric structures of *N*-salicylidene-*p*-X-aniline–methanol hydrogen bonded complex for the enol and keto configurations, determined from the AM1 method and *ab initio* with HF/3-21G method.

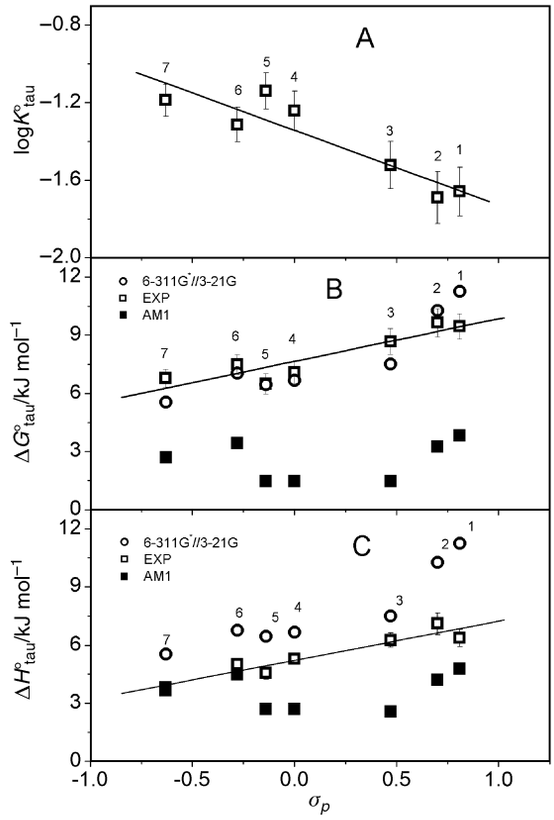

Fig. 4 A. Linear correlation of log K_{tau} against σ_p Hammett parameters. B. Linear correlation of ΔG°_{tau} against σ_p Hammett parameters. C. Linear correlation of ΔH°_{tau} against σ_p Hammett parameters.

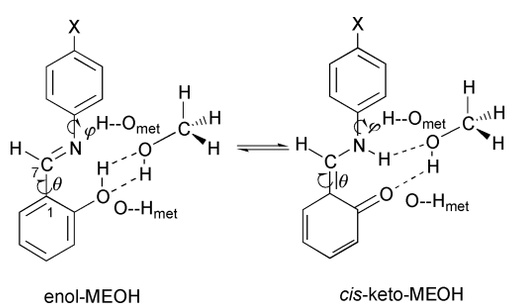

Fig. 5 Intermolecular hydrogen bonding of *N*-salicylidene-*p*-X-anilines with a methanol molecule, for enol and keto tautomers.

The formation energy of each hydrogen bonded solute–solvent complex, for the enol–methanol (ΔE_{ehb}) and keto–methanol (ΔE_{khb}) tautomeric species, is given by eqns. (5) and (6), respectively.

$$\Delta E_{ehb} = E_{ehb} - (E_e + E_{met}) \qquad (5)$$

$$\Delta E_{khb} = E_{khb} - (E_k + E_{met}) \qquad (6)$$

E_{ehb} and E_{khb} are the total energies of the fully optimized hydrogen-bonded complexes of the enol and keto forms,

Table 2 AM1 Heat of formation and 6-311G*//3–21G MO energy calculations for enol (e) and keto (k) *N*-salicylidene-*p*-X-aniline and *N*-salicyl-*p*-X-aniline–methanol hydrogen bond complexes (hb)

	AM1/kJ mol^{-1}	6-311G*//3-21G[a]/au
E_e	121.75	−627.880314
$E_e + E_{met}$	−116.98	−742.887668
E_{ehb}	−129.66	−742.902068
$\Delta E_{ehb} = E_{ehb} - (E_e + E_{met})$	−12.63	−0.0144
		37.81 kJ mol^{-1}
E_k	140.37	−627.869401
$E_k + E_{met}$	−98.32	−742.876755
E_{khb}	−126.98	−742.899528
$\Delta E_{khb} = E_{khb} - (E_k + E_{met})$	−28.66	−0.0228
		−59.79 kJ mol^{-1}

[a] The *ab initio* calculation including the ZPE thermal corrections.

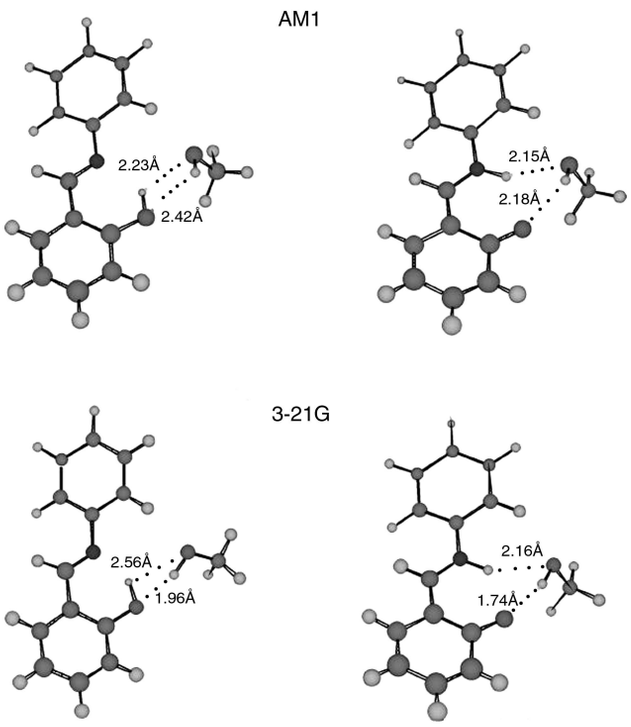

Fig. 6 Optimized geometrical structures obtained from AM1 and *ab initio* calculations.

respectively. E_e and E_k are the total energies of the optimized geometry of the non-bonded enol and keto forms and E_{met} is the energy of the optimized geometry of a methanol molecule.

To compare the AM1 and *ab initio* results, we have added, in *ab initio* calculations, the thermal ZPE correction enthalpy,[18,19] at 298.15 K to the total energy. This is a standard procedure, and requires calculation of the force field. With the knowledge of the force field and the moments of inertia even the calculation of the partition function and the thermodynamic data at room temperature is straightforward.[20] The standard enthalpy of the enol→keto tautomeric reaction is given by $\Delta H^\circ_{tau} = E_k - E_e$ for the non-bonded fragment and $\Delta H^\circ_{tau}(hb) = E_{khb} = E_{ehb}$ for the H-bonded complex.

In Table 2 we display the AM1 and 6-311G*//3-21G results of *N*-salicylidene-*p*-X-aniline and the *N*-salicylidene-*p*-X-aniline–methanol hydrogen-bonded complexes. We note that the formation energy of the keto–methanol complex (E_{khb}) is higher than the formation energy of the enol–methanol complex (E_{ehb}). This higher stabilization energy of the keto complex reduces the ΔH°_{tau} value, from 18.6 to 2.7 kJ mol^{-1} in AM1, and from 28.7 to 6.7 kJ mol^{-1} in the *ab initio* calculation. The energy values are in agreement with the absorption and fluorescence excitation spectra shown in Fig. 2. In cyclohexane it is not possible to observe the visible band at 450 nm associated with the keto species, which is probably due to the fact that in a non-polar solvent the energy between both species is about 20 kJ mol^{-1} or more. The equilibrium should then be shifted to the enol form and the absorption spectra should present only the one band associated with this species. On the other hand, in a protic solvent, the energy difference is reduced to 4 kJ mol^{-1}, and a small fraction of the keto species is present in the solution, and therefore a weak absorption band in the visible region appears.

Table 3 AM1 (first row) and 6-311G*//3-21G (second row) standard thermodynamic properties calculations, variation of the phenylaniline dihedral angle, $\Delta\varphi^\circ$, and absolute dipole moment changes, $\Delta\mu$, for the tautomeric reaction of the *N*-salicylidene-*p*-X-aniline–methanol hydrogen bond complexes

	ΔG°_{tau}	ΔH°_{tau}	$T\Delta S^\circ_{tau}$	$\Delta\varphi^\circ(\varphi_{keto})$[a]	$\Delta\mu$/debye[b]
-NMe_2	2.702	3.653	0.825	−7.4 (26.5)	2.637
	5.916	5.535	−0.525	−4.0 (22.6)	2.332
-OMe	3.414	4.485	1.148	−3.1 (28.8)	2.250
	7.739	7.037	−0.605	2.0 (19.5)	1.792
-Me	1.452	2.686	0.792	4.1 (21.7)	1.954
	7.142	6.452	−1.045	9.4 (18.6)	1.389
-H	1.464	2.686	0.794	5.4 (21.5)	1.618
	7.167	6.661	−0.805	10.3 (19.0)	1.018
-COMe	1.460	2.569	0.680	12.8 (17.5)	1.222
	8.217	5.828	−0.996	18.7 (11.7)	1.170
-CN	3.243	4.201	0.961	12.7 (13.6)	1.393
	11.180	10.263	−2.247	19.1 (11.8)	1.028
-NO_2	3.807	4.778	1.108	18.8 (12.8)	−1.279
	12.247	11.255	−2.554	24.3 (9.3)	−0.835

[a] HF/3-21G calculations. [b] HF/6-311G*//3-21G calculations.

Thermodynamics calculations. For each compound under study, we have calculated the total energy for the optimized hydrogen bonded complex of the enol and keto species. In the evaluation of the thermodynamics properties H°(hb), G°(hb) and S°(hb), we have used the option "thermo"[21] and "frequency"[19] in both AM1 and *ab initio*, calculations, respectively. For the enol-imine→keto-amine tautomeric reaction, the standard properties (ΔP°_{tau}(hb)), were evaluated through ΔP°_{tau}-(hb) = P°(khb) − P°(ehb), where P° represents any thermodynamic property, H°, G°, S°.

In Table 3, we present the calculated ΔG°_{tau}(hb), ΔH°_{tau}(hb) and $T\Delta S^\circ_{tau}$(hb) values for the tautomeric reaction at 298 K. We observe that ΔG°_{tau}(hb) and ΔH°_{tau}(hb) values, calculated by means of the 6-311G*//3-21G basis (second row), are systematically larger than the AM1 ones (first row). The greatest difference between them was found in the nitro-substituted compound.

In order to compare the calculated thermochemical properties with the experimental ones, we show in Figs. 4-B and 4-C the calculated and experimental values against the Hammett parameter. In Fig. 4-B we show the 6-311G*//3-21G ΔG°_{tau}(hb) values. They are quite close to the experimental data with a small negative deviation of 0.13 kJ mol^{-1} (on average). On the other hand, the AM1 results present a larger negative deviation of −5.4 kJ mol^{-1} (on average) with respect to the experimental data, which is due to the positive value of the calculated entropic contribution (see Table 3).

The AM1 and *ab initio* ΔH°_{tau}(hb) values are shown in the Fig. 4-C. It can be seen that the AM1 calculations display a negative deviation (1.9 kJ mol^{-1} on average) and the *ab initio* values predict a positive deviation (2.3 kJ mol^{-1}, on average), with respect to the experimental values. Furthermore, we note that the *ab initio* data follow the same trend with a good linear correlation ($r = 0.94$). In contrast to this, the AM1 results do not exhibit an important effect of the substituent, leading to a poor linear correlation ($r = 0.25$).

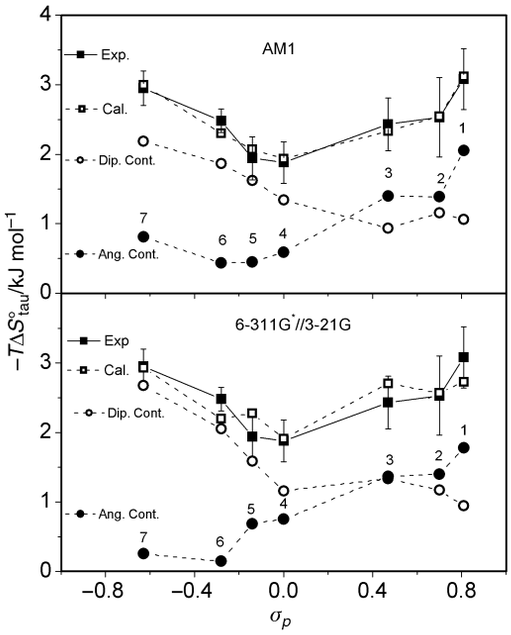

Fig. 7 Calculated angular and dipole contributions to $T\Delta S^{\circ}$ experimental values.

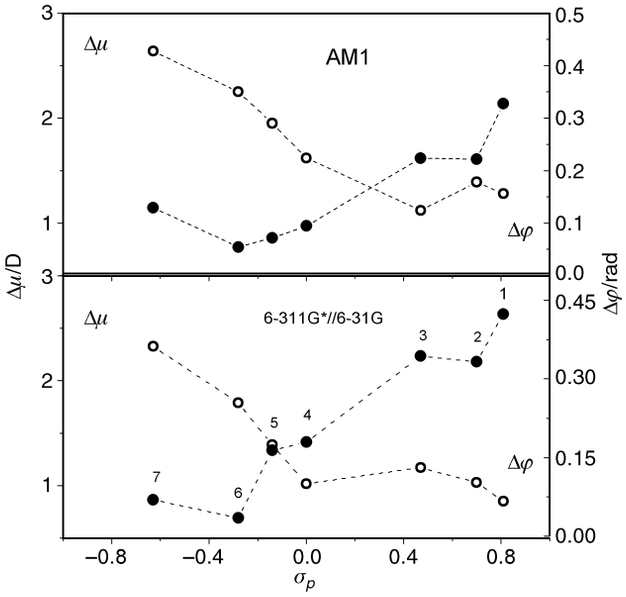

Fig. 8 Plot of the calculated AM1 and 6-311G*//3-21G $\Delta\varphi$; and $\Delta\mu$ values against σ_p Hammett parameters.

Entropy calculation model. Fig. 7 displays $-T\Delta S^{\circ}_{tau}$ values at 298 K against σ_p. It is observed that the species with higher values of σ_p (*i.e.*, species **1** and **7**, at both extremes of the figure) present the higher $T\Delta S^{\circ}$. These values are dependent only on the absolute σ_p, and decrease towards a minimum for X = H. To explain this trend, we propose a model based on the structural changes occurring in the solute when the tautomeric reaction takes place (*vide supra*).

In our *N*-salicylidene-*p*-X-aniline compounds there are two molecular parameters that change considerably during the tautomeric equilibrium. These are the angle φ (see Fig. 1) and the dipole moment $|\vec{\mu}|$. To quantify the structural molecular changes in the intramolecular proton process, we define the change of the dihedral angle as $\Delta\varphi = \varphi_{keto} - \varphi_{enol}$ and the change of the dipole moment as $\Delta\mu = |\overrightarrow{\mu_{keto}}| - |\overrightarrow{\mu_{enol}}|$. Therefore $\Delta\mu$ and $\Delta\varphi$ can be seen as a measure of the intramolecular charge transfer and the molecular geometry change, respectively, when the intramolecular proton transfer takes place. Furthermore, both variables are dependent on the electronic acceptor or donor nature of substituent in the phenylaniline ring.

In Table 3 we present the $\Delta\varphi$ and $\Delta\mu$ values calculated with AM1 and 3-21G methods. Both calculations lead to similar trends for the $\Delta\varphi$ and $\Delta\mu$ variables. In Fig. 8 we display the plot of $\Delta\varphi$ and $\Delta\mu$ *versus* σ_p. These show that $\Delta\varphi$ increases when the electron acceptor properties of the substituent increase. Furthermore, $\Delta\mu$ increases when the electron donor properties increase from nitro- to dimethylamine-substituted compounds.

In the enol-imine→keto-amine reaction in our molecular system in methanol solution, the $T\Delta S^{\circ}$ value is a measure of the reorganization of methanol molecules around the solute. This reorganization in the solvent is induced by changes in the solute molecular properties when the enol→keto reaction takes place.

The above results suggest that the experimental $T\Delta S^{\circ}_{tau}$ values contain two contributions: one electronic, probably proportional to the dipole change ($\Delta\mu$), and the other a geometric contribution, dependent on the dihedral angle change ($\Delta\varphi$): Therefore the experimental values of $T\Delta S^{\circ}_{tau}$ may be expressed through eqn. (7), where a and b are coefficients obtained by

$$-T\Delta S = a\Delta\mu + b\Delta\varphi \qquad (7)$$

means of multiple linear regression. We have obtained $a = -0.83\pm0.05$ kJ mol^{-1} debye^{-1}, $b = -6.27\pm0.40$ kJ mol^{-1} rad^{-1} ($r = 0.99$) at the AM1 level and $a = -1.15\pm0.16$ kJ mol^{-1} debye^{-1}, $b = -4.20\pm0.69$ kJ mol^{-1} rad^{-1} ($r = 0.94$) at the 6-311G*//3-21G level.

Knowledge of the coefficients a and b allows us to calculate separately the dipole and angular change contributions to the total entropy change in the enol→keto reaction. Fig. 7 displays both contributions to $-T\Delta S^{\circ}$.

Conclusions

The high sensitivity of the fluorescence technique allows accurate determination of the tautomeric constants for the enol→keto reaction of the *N*-salicylidene-*p*-X-aniline compounds in methanol solution.

The hydrogen bond in *N*-salicylidene-*p*-X-aniline derivatives with a methanol solvent molecule, characterized by means of MO calculations, has been shown to be an adequate model to explain the absorption and the fluorescence excitation spectra of *N*-salicylidene-*p*-X-aniline in methanol solution.

The thermodynamic standard properties of *N*-salicylidene-*p*-X–aniline–methanol complexes, determined by means of AM1 and *ab initio* MO calculations are in good agreement with the experimental values. However, the semiempirical AM1 method results inadequately account for the effect of substituents.

When the enol→keto tautomeric reaction takes place, the entropy changes in the molecular salicylidene species are correctly described by means of a linear function of the $\Delta\varphi$ and $\Delta\mu$ molecular parameters.

Acknowledgements

The authors acknowledge the FONDECYT Project 1970787 for financial support. We also appreciate helpful comments from Professors Alejandro Toro-Labbé and Raúl. G. E. Morales.

References

1 S. M. Ormsom and R. G. Brown, *Prog. React. Kinet.*, 1994, **19**, 45.
2 A. J. G. Stranjord, D. E. Smith and P. F. Barbara, *J. Phys. Chem.*, 1985, **89**, 2362.
3 J. Catalan and J. C. Valle, *J. Am. Chem. Soc.*, 1992, **115**, 4321.
4 M. I. Knyazhansky, A. V. Metelitza, A. J. Buskov and S. M. Aldoshim, *J. Photochem. Photobiol. A.*, 1996, **97**, 121.

5 K. Ogawa and T. Fujiwara, *Chem. Lett.*, 1999, 667.
6 L. Antonov, W. M. F. Fabian, D. Nedelcheva and F. S. Kamounah, *J. Chem. Soc.*, *Perkin Trans. 2*, 2000, 1173.
7 E. Hadjoudis, *Mol. Eng.*, 1995, **5**, 301.
8 S. R. Salmam, R. D. Ferrant and J. C. Lindon, *Spectrosc. Lett.*, 1991, **24**, 1071.
9 S. H. Alarcón, A. C. Oliveri and M. González-Sierra, *J. Chem. Soc.*, *Perkin Trans. 2*, 1994, 1067.
10 J. R. Lakowicz, *Principles of Fluorescence Spectroscopy*, Plenum Press, New York, 1983.
11 M. Dewar, E. Zoebisch, E. Healy and J. Stewart, *J. Am. Chem. Soc.*, 1985, **107**, 3902.
12 WinMopac 2.0, Fujitsu Limited, 1997–1998.
13 Gaussian 98, Revision A.7, M. J. Frisch, G. W. Trucks, H. B. Schlegel, G. E. Scuseria, M. A. Robb, J. R. Cheeseman, V. G. Zakrzewski, J. A. Montgomery, Jr., R. E. Stratmann, J. C. Burant, S. Dapprich, J. M. Millam, A. D. Daniels, K. N. Kudin, M. C. Strain, O. Farkas, J. Tomasi, V. Barone, M. Cossi, R. Cammi, B. Mennucci, C. Pomelli, C. Adamo, S. Clifford, J. Ochterski, G. A. Petersson, P. Y. Ayala, Q. Cui, K. Morokuma, D. K. Malick, A. D. Rabuck, K. Raghavachari, J. B. Foresman, J. Cioslowski, J. V. Ortiz, A. G. Baboul, B. B. Stefanov, G. Liu, A. Liashenko, P. Piskorz, I. Komaromi, R. Gomperts, R. L. Martin, D. J. Fox, T. Keith, M. A. Al-Laham, C. Y. Peng, A. Nanayakkara, C. Gonzalez, M. Challacombe, P. M. W. Gill, B. Johnson, W. Chen, M. W. Wong, J. L. Andres, M. Head-Gordon, E. S. Replogle and J. A. Pople, Gaussian, Inc., Pittsburgh PA, 1998.
14 R. G. E. Morales, G. P. Jara and V. Vargas, *Spectrosc. Lett.*, 2001, **34**, 1.
15 G. Dudek and E. P. Dudek, *J. Chem. Soc. B*, 1971, 1356.
16 C. D. Johnson, *The Hammett Equation*, Cambridge University Press, 1980, pp. 1–9.
17 J. March, *Advanced Organic Chemistry*, 4th edn., J. Wiley & Sons, 1992, p. 280.
18 J. B. Foresman and Æ. Frisch, *Exploring Chemistry with Electronic Structure Methods*, 2nd edn., 1996, Gaussian, Inc., Pittsburg, P.A., pp. 68, 125 and 169.
19 Gaussian 98, User's Reference, Gaussian, Inc., p. 77.
20 W. Kutzelnigg, *J. Mol. Struct. (THEOCHEM)*, 1988, **181**, 33.
21 MOPAC 93 Manual, Revision Number 2, Fujitsu Limited, 1997–1998.